

ScienceDirect



IFAC PapersOnLine 56-3 (2023) 193-198

Modeling the Impact of Animal Size on the Effectiveness of Peritoneal Oxygenation

Grace M. Sarkar* Anna E. Shaw** Hosam K. Fathy***

* Student, Neurobiology & Physiology, Univ. of Maryland.

** Student, Cell Biology & Genetics, Univ. of Maryland.

*** Professor, Mechanical Eng., Univ. of Maryland (Author emails:
gsarkar@terpmail.umd.edu, ashaw127@terpmail.umd.edu,
hfathy@umd.edu (corresponding author)).

Abstract: This paper develops a scalable model of the dynamics of gas exchange during peritoneal oxygenation, motivated by the potential of such oxygenation to provide life support for patients with severe respiratory failure. The literature presents peritoneal oxygenation experiments for both large and small animals, including adult swine, rabbits, rats, and piglets. Results of these experiments suggest a potential discrepancy, with the benefits of peritoneal oxygenation possibly being stronger for smaller animals. We hypothesize that this size dependence is at least partially attributable to the effect of animal size on the ratio of peritoneal diffusion surface area to animal volume. The paper develops a scalable multi-compartment model of gas transport dynamics during peritoneal oxygenation. Simulating this model provides important insights regarding the potential impact of animal size on the viability of peritoneal oxygenation.

Copyright © 2023 The Authors. This is an open access article under the CC BY-NC-ND license (https://creativecommons.org/licenses/by-nc-nd/4.0/)

Keywords: Peritoneal oxygenation; multi-compartment modeling; gas transport dynamics.

1. INTRODUCTION

This paper aims to compare peritoneal oxygenation between adult pigs and piglets using a scalable model to simulate the dynamics of gas exchange. Specifically, this research simulates the impact of the peritoneal surface area to volume ratio on the dynamics of gas transport. Overall, identifying the impact of animal size on peritoneal oxygenation has the potential to guide experiments on this treatment in both adult or neonate patients in the future.

Mechanical ventilation (MV) and extracorporeal membrane oxygenation (ECMO) are currently the main means used to oxygenate patients in severe respiratory failure (Ohshimo (2021)). However, these oxygen delivery methods are both invasive and costly. MV in the ICU costs approximately \$1,522 per day (Dasta et al. (2005)). The mean estimated cost for ECMO was \$73,122 in 2010. reaching an average of \$213,246 with pre- and post-care costs (Mishra et al. (2010)). Studies conducted by the CDC have approximated that more than 300,000 patients receive MV in the United States each year (Wunsch et al. (2010)). These patients are at high risk for complications and poor outcomes including ventilator-associated pneumonia (VAP), sepsis, acute respiratory distress syndrome (ARDS), ventilator-induced lung injury (VILI), pulmonary embolism, barotrauma, pulmonary edema, and death. Overall, the invasiveness of MV can lead to longer hospital durations and more expensive hospital bills (Haribhai and Mahboobi (2022)). The literature estimates that mortality in patients with acute lung injury on MV ranges from 24% in 15 to 19-year-olds to 60% for patients 85 years and older (Rubenfeld et al. (2005)). Additionally, 100,000 persons per year were placed on ECMO from 2011

to 2014 (Stentz et al. (2019)). Patients placed on ECMO are at high risk of bleeding, infection, thrombosis, and death (Teijeiro-Paradis et al. (2022)).

Invasive respiratory support is commonly used not just for adult patients, but also for neonates. In 2012, 82% of infants who were born before 29 weeks of gestation were put on MV (Klingenberg et al. (2017)). As of 2021, over 45,000 neonates rely on ECMO worldwide, amounting to 27% of all ECMO patients (Rycus and Stead (2022)). For neonatal patients on MV, one study found a mortality rate of 43% (Iqbal et al. (2015)), plus additional complications mirroring those in adults. For neonatal patients on ECMO, the reported mortality rate in a retrospective analysis was 35% (Reiterer et al. (2018). One notable difference between complications of ECMO for adults and neonates is the increased risk of hemorrhage and thrombosis due to the underdeveloped hemostatic systems of neonatal patients. This puts them at an increased risk of morbidity/mortality, and requires specialized personnel to operate (Van Ommen et al. (2018)).

The need for patients to be placed on MV increased rapidly during the SARS-CoV-2 pandemic. During the peak of the pandemic, approximately 10-20% of patients admitted to the hospital in the United States and Europe with SARS-CoV-2 were placed on MV (Grasselli et al. (2021)). During the pandemic, one ICU study showed that 4,044 out of 58,472 patients were placed on ECMO (Bertini et al. (2022)).

Given the cost and risks of MV and ECMO, the literature is exploring other means of oxygen delivery in animal trials, including peritoneal oxygenation (Carr et al.

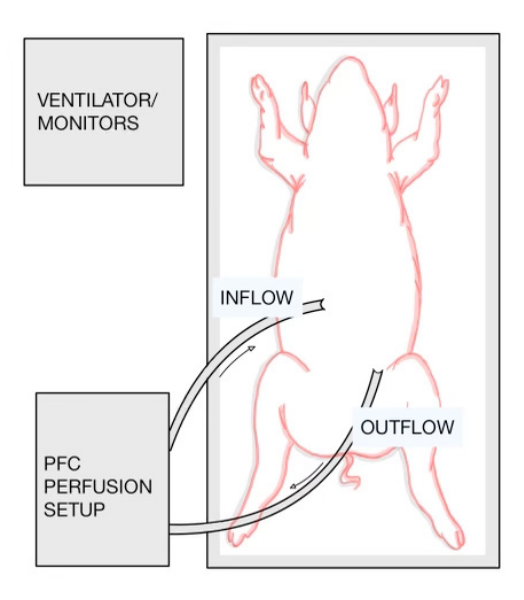


Fig. 1. Peritoneal perfusion schematic with PFC

(2006)). This is a form of liquid ventilation that uses a gas carrier, like perfluorocarbons (PFCs) or oxygen microbubbles (OMBs), to improve the gas exchange capacity of diseased lungs. An example schematic of perfusion with PFCs in laboratory swine is shown in Fig.1. Analogous to peritoneal dialysis, the gas carrier liquid is pumped into the peritoneal (i.e., abdominal) chamber where oxygen then diffuses into the patient's bloodstream (Carr et al., 2006; Feshitan et al., 2014). This paper focuses specifically on peritoneal oxygenation using PFCs: inert, nontoxic, fluorine-based organic compounds that are effective at dissolving gas (Carr et al. (2006)).

Multiple studies suggest that peritoneal oxygenation using different gas carriers increases the mean survival time of smaller laboratory animals like hypoxic rats and rabbits (Klein et al., 1986; Matsutani et al., 2010; Zhang et al., 2010; Barr et al., 1994, 1996). However, the literature also suggests that peritoneal gas transport may be slower, and therefore less impactful, in larger vs. smaller laboratory animals. Feshitan, et al., for instance, found success in the peritoneal oxygenation of laboratory rats using OMBs (Feshitan et al. (2014)), but less success was seen in the application of the same technique to laboratory swine (Mohammed et al. (2022)). This suggests that animal size impacts the effectiveness of peritoneal oxygenation.

The area of the peritoneal membrane changes with animal size, with larger animals exhibiting a smaller area to volume ratio (Fischbach et al. (2005)). This can potentially have a negative impact on diffusion rates, thereby limiting the overall effectiveness of peritoneal oxygenation (Gallet et al. (2017)). Unfortunately, to the best of the authors' knowledge, the problem of using dynamic simulation models to study the impact of animal size on the effectiveness of peritoneal oxygenation remains unexplored.

The goal of this paper is to address the above research gap by making three contributions to the literature. First, the paper postulates a scalable model of peritoneal oxygenation dynamics in laboratory swine. Key scaling laws in this model are obtained from the literature, allowing the model to simulate peritoneal oxygenation dynamics in both adult and infant animals (Section 2). Second, the paper parameterizes this model based on the literature, leading to a model with physiologically plausible parameters (Section 2). Third, the paper simulates this model for a number of virtual hypoxia and peritoneal oxygenation experiments corresponding to different laboratory animal sizes (Section 3). This simulation shows, for the first time, that peritoneal oxygenation has the potential to be more than 3 times as effective for infant laboratory swine compared to adult swine. This provides an important potential explanation for key existing experimental findings in the peritoneal oxygenation literature, and can serve as a foundation for potential future research on improving the efficacy of this medical intervention. Finally, Section 4 summarizes the paper's conclusions.

2. MODEL DEVELOPMENT

The remainder of this paper analyzes a model of gas exchange dynamics containing four compartments, namely: the lungs, the peritoneal vasculature, the remaining systemic vasculature, and the volume of PFC retained within the body. The model has four state variables, namely:

- (1) The partial pressure of oxygen in the lung compartment, $x_1(t)$ [mmHg].
- (2) The percentage oxygen in the peritoneal vasculature compartment, x₂(t) [−].
- (3) The percentage oxygen in the remaining vasculature compartment, $x_3(t)$ [-].
- (4) The percentage of oxygen dissolved in the PFC retained within the body (relative to the maximum oxygen that can be dissolved in PFC).

These variables were chosen due to their significance in peritoneal perfusion. This method focuses on the transport of dissolved oxygen from the abdominal cavity through the peritoneum and into the bloodstream, ultimately reoxygenating the blood while easing stress on the lungs (Feshitan et al., 2014). Therefore, the lungs, the dissolved oxygen in the PFC, and the vasculature of the peritoneum and the body are all critical to the model. Both vasculature compartments are assumed to represent venous blood oxygen saturations. Moreover, the model assumes that x_1 represents an alveolar oxygen partial pressure, which is further assumed to be a good approximation of the oxygenation of both the systemic arteries and pulmonary veins. Therefore, the animal's pulse oximetry can be computed from x_1 using the Hill equation's dissociation function:

$$f_d(x) = 100 \frac{\left(\frac{x_1}{P_{50}}\right)^r}{1 + \left(\frac{x_1}{P_{50}}\right)^r} \tag{1}$$

where p_{50} is the partial pressure of oxygen at 50% saturation and r is a constant governing the steepness of the hemoglobin dissociation curve (Leow (2007)).

In addition to the above state variables, the model has four control inputs, namely:

- The laboratory animal's minute ventilation rate, *u*₁(*t*) [*L.min*⁻¹].
- (2) The fraction of inspired oxygen (FiO2), $u_2(t)$ [-].
- (3) The PFC perfusion flowrate, $u_3(t)$ [L.min⁻¹].
- (4) The percentage of oxygen dissolved in the PFC inflow to the animal, u₄(t) [mmHq].

Based on the above definitions, the proposed model consists of the following three scalable state equations:

$$\begin{split} \frac{s_l^3 V_1 \dot{x}_1}{P_{atm} - P_{H_2O}} &= (s_l^3 u_1) \left(u_2 - \frac{x_1}{P_{atm} - P_{H_2O}} \right) \\ &- \frac{\alpha s_l^3 Q H}{100} (f_d(x_1) - x_2) \\ &- \frac{(1 - \alpha) s_l^3 Q H}{100} (f_d(x_1) - x_3) \\ s_l^3 V_2 H \frac{\dot{x}_2}{100} &= \frac{\alpha s_l^3 Q H}{100} (f_d(x_1) - x_2) \\ &- \alpha s_l^3 w \\ &+ \frac{k A s_l^2}{100 s_l T} (x_4 - x_3) \\ s_l^3 V_3 H \frac{\dot{x}_3}{100} &= \frac{(1 - \alpha) s_l^3 Q H}{100} (f_d(x_1) - x_3) \\ &- (1 - \alpha) s_l^3 w \\ s_l^3 V_4 \gamma \dot{x}_4 &= u_3 s_l^3 \gamma (u_4 - x_4) \\ &- \frac{k A s_l^2}{100 s_l T} (x_4 - x_3) \end{split}$$

The above state equations can be obtained using the principle of conservation of mass, where every term in the equations represents an oxygen transport or consumption rate, in liters per minute (at standard atmospheric conditions). In these equations, s_l is a length scale factor, representing the size of the given laboratory animal. Compartment volumes, metabolic oxygen consumption rates, minute ventilation, and cardiac output are all assumed to be functions of the cube of this scale factor, s_I^3 . Diffusion surface area and the thickness of the diffusion layer, in contrast, are assumed to be functions of s_l^2 and s_l , respectively. The symbols $V_{1,\dots,4}$ represent the volumes of all four compartments, in liters, and are approximated as constant. Treating V_4 , in particular, as constant corresponds to neglecting the filling and emptying of the peritoneal cavity: an assumption that can easily be relaxed in future work by making V_4 a fifth state variable. The terms P_{atm} and P_{H_2O} refer, respectively, to atmospheric pressure and tracheal water vapor pressure, in mmHg. The multipliers α and $1 - \alpha$ represent the fractions of systemic blood flow to the peritoneal vasculature and the remaining systemic vasculature, respectively. The total rate of oxygen consumption due to metabolism, in liters of oxygen per second, is denoted by w, and assumed to be split among the different vasculature compartments in the same ratio as blood flow. The symbol Q refers to cardiac output (i.e., blood flow), in liters per minute, and H is a conversion factor that converts percent oxygen saturation in the vasculature to liters of dissolved oxygen per liter of blood. In other words, H is essentially a solubility

constant. The effective volumetric diffusion rate through the peritoneal lining is assumed to be governed by Fick's law of diffusion, where k is an effective diffusivity constant, A is the peritoneal surface area, and T is the peritoneal diffusion distance. It is important to note that this model does not consider any physiological characteristics that may differ between adult and infant swine other than surface area to volume ratios.

The parameters for the above model are listed in Table 1. Due to the resemblance in physiology and morphology between adult swine and adult humans, particularly in the structure and function of the cardiovascular system and gastrointestinal tract (Walters and Prather (2013), parameters that did not have supporting literature for adult swine were assigned values for adult humans. Values were obtained from several sources, including Zosky (2015), Solass et al. (2019), van Gelder et al. (2020), Stewart and Montgomery (2005), Mahon et al. (2019), Cameron et al. (2007), Rhodes and Varacallo (2019), Van Milgen et al. (1997), Albanese et al. (2009), Abrahams et al. (2019), Jägers et al. (2021), Collins et al. (2015), Hatoum (2016), and Katakam (2022).

Table 1. Parameters (AS-Adult Swine, AH-Adult Human)

Symbol	Meaning	Value/Units
V_1	Pulmonary vol. $_{AS}$	4.775L
V_2	Blood vol. to peritoneal cavity $_{AH}$	1.789L
V_3	Blood vol. in remainder of $body_{AS}$	1.94L
V_4	Vol. of PFC in peritoneal cavity $_{AS}$	2.5L
P_{atm}	Atmospheric pressure	760mmHg
P_{H2O}	Partial pressure of H2O	23.8mmHg
α	Fraction Q to peritoneal cavity $_{AH}$	32% Q
Q	Cardiac output $_{AS}$	6.07 L/min
H	Liters oxygen per liter $blood_{AS}$	$0.21LO_{2}$
W	Oxygen metabolism $_{AS}$	0.30 L/min
A	Peritoneal area $_{AH}$	$1.43m^2$
T	Peritoneal thickness $_{AH}$	$113\mu m$
γ	Liters of O2 dissolved in 1L PFC	$0.403LO_{2}$
P_{50}	P_{H2O} 50% hemoglobin dissociation	26mmHg
r	Hill eq. hemoglobin coefficient	2.8
k	Diffusivity constant _{AH}	$1.7E-5 \ cm^2/s$
u_1	Minute ventilation $_{AS}$	5L air/min
u_2	Fraction of inspired O_{2AS}	0.21, 0.11
u_3	PFC perfusion $rate_{AS}$	3.5 L/min
u_4	PFC O2 saturation	100%
$x_1(0)$	Initial condition for $x_1(t)$	104mmHg
$x_2(0)$	Initial condition for $x_2(t)$	90%
$x_3(0)$	Initial condition for $x_3(t)$	90%
$x_4(0)$	Initial condition for $x_4(t)$	100%

3. RESULTS AND ANALYSIS

Four simulation studies were performed using the above model and parameters. The total duration of each simulation study was 60 minutes: (i) 20 minutes of normoxia with an inspired oxygen levels of 21% and no perfusion; then (ii) 20 minutes of hypoxia at a reduced inspired oxygen level; then finally (iii) 20 minutes of hypoxia plus perfusion at a steady volumetric perfusate flowrate. All simulations were performed using OpenModelica. The intent of the three phases of each simulation study were to first establish a steady-state, equilibrium state of normoxia, then to establish steady-state hypoxia, then finally to examine the

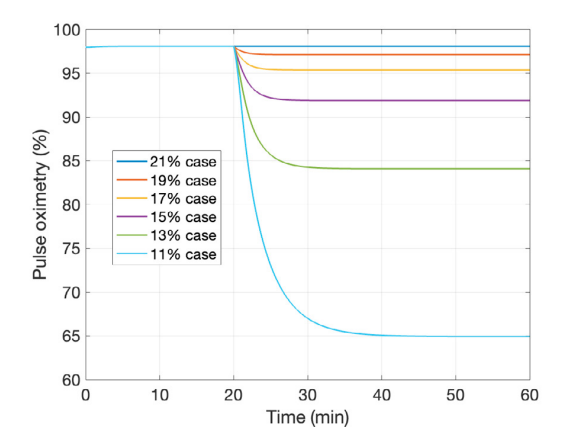


Fig. 2. Adult swine simulation, varying hypoxia levels

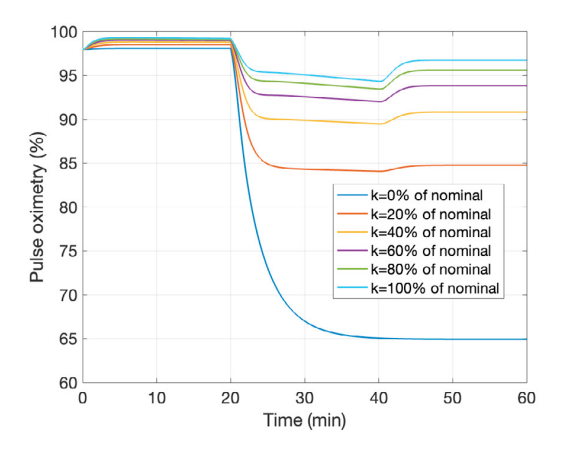


Fig. 3. Adult swine simulation, varying diffusivities

impact of perfusion. Each of the four studies examined the effect of a different simulation parameter, as explained below.

Fig. 2 shows the pulse oximetry results of the first simulation study, where different levels of normoxia were induced for an adult swine ($s_l=1$) by changing the inspired oxygen fraction. The perfusion flowrate was zero throughout this study. The goal was to study the degree to which different levels of inspired oxygen affect hypoxia in an adult swine. The results of this simulation are consistent with the hemoglobin dissociation equation, where a very rapid decline in pulse oximetry occurs between the 13% and 11% inspired oxygen levels. This is an important baseline study highlighting the fact that the proposed model produces intuitive results, consistent with the hypoxia literature.

Fig. 3 shows the pulse oximetry try results of the second simulation study, where the inspired oxygen fraction was always set to 11% during hypoxia, the perfusion flowrate was always set to 3L/min., but different values of peritoneal diffusivity, k, were simulated for an adult swine $(s_l=1)$. The goal was to study the impact of peritoneal diffusivity on the effectiveness of peritoneal oxygenation, for 0%, 20%, 40%, 60%, 80%, and 100% of the nominal value in Table 1. The results of this simulation show significant success in animal recovery from hypoxia due to

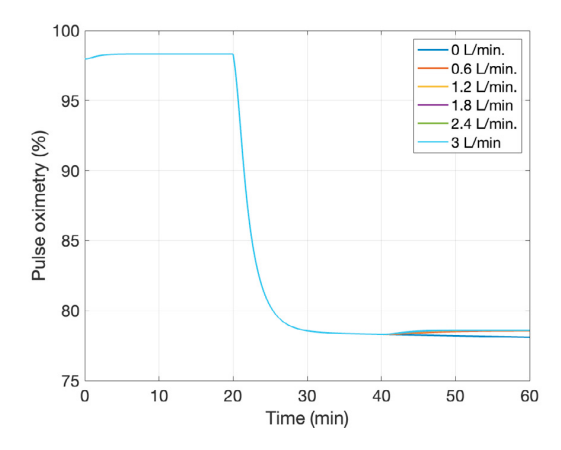


Fig. 4. Adult swine simulation, varying flowrates

peritoneal oxygenation. Interestingly, the improvement in animal pulse oximetry begins quite early in the simulation, reflecting the fact that the perfusate already stored in the peritoneal cavity is replenishing the animal's blood oxygen from the onset of the experiment. This suggests a potential benefit to "dwell" experiments, where an initial bolus of PFC is supplied to the animal and allowed to dwell prior to the onset of hypoxia. The results of this simulation are quite positive, perhaps to the point of being optimistic. This could potentially be due to an optimistic nominal estimate of diffusivity or the thickness of the peritoneal tissue lining: two parameters that may not be easy to estimate. In this simulation, decreasing the diffusivity constant would impact the results similarly to increasing the peritoneal thickness. With this in mind, the next two scenarios will assume a conservative value for peritoneal diffusivity, k - namely, 10% of its nominal value from Table

Fig. 4 shows the pulse oximetry results of the third simulation study, where the inspired oxygen fraction was always set to 11% during hypoxia, peritoneal diffusivity was always set to 10% of its nominal value from Table 1, but different peritoneal perfusion flowrates were used for an adult swine ($s_l=1$). The goal was to study the impact of perfusion flowrate on perfusion effectiveness, for 0%, 20%, 40%, 60%, 80%, and 100% of the nominal perfusion flowrate. The impact of perfusion flowrate on pulse oximetry is quite small, suggesting that peritoneal oxygenation is a diffusion-limited, rather than perfusion-limited, process. This is an important potential insight for future research on the refinement of peritoneal oxygenation.

Finally, Fig. 5 shows the impact of animal size on pulse oximetry during a combined hypoxia/perfusion study where the inspired oxygen fraction was always set to 11% during hypoxia, peritoneal diffusivity was always set to 10% of its nominal value from Table 1, and the perfusion flowrate u_3 was always set to 3L/min for a full-size animal (but scaled with animal size based on the simulation model). The goal was to study the impact of animal size on perfusion effectiveness, for values of s_l equal to 1.0, 0.9, 0.8, 0.7, 0.6, and 0.5. For a nominal adult swine mass of 55kg, setting $s_l = 1$ maintains this mass, while setting $s_l = 0.5$ corresponds to a piglet of mass 55/8 = 6.874kg. The results of this simulation study show a dramatic im-

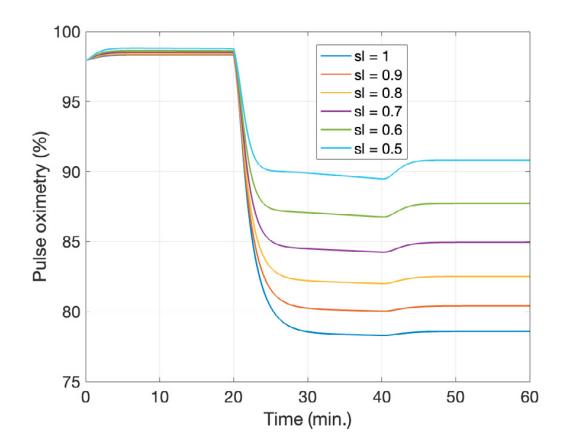


Fig. 5. Adult swine simulation, varying animal sizes

provement in peritoneal oxygenation for a smaller animal size. Specifically, for an adult pig of 55kg mass, peritoneal oxygenation fails in bring pulse oximetry above the 80% mark. In contrast, for a piglet of 6.875kg mass, peritoneal oxygenation succeeds in bringing pulse oximetry above the 90% mark. This is consistent with the existing literature on peritoneal oxygenation, which suggests that peritoneal oxygenation is significantly more effective for smaller animals. For human patients, this raises the possibility that peritoneal oxygenation may be significantly more effective for neonatal, as opposed to adult, patients.

4. CONCLUSION

Overall, our model results demonstrate that there is a notable difference between the peritoneal oxygenation of adult swine and piglets using PFC. This supports the hypothesis that discrepancies in the surface-area-to-volume ratio between adult swine and piglets significantly impact the efficacy of peritoneal perfusion with PFC. Further model analysis and animal trials are needed to confirm this preliminary, simulation-based result and to consider the impact of other physiological differences between infant and adult swine. Based on this model, future research can potentially be conducted to mathematically quantify the difference in peritoneal oxygenation of adult swine versus piglets when changing hypoxia levels, perfusion flowrates, peritoneal diffusivities, and animal size. Additionally, a maximum size value could potentially be determined for using peritoneal oxygenation as successfully as MV and ECMO.

ACKNOWLEDGEMENTS

The authors gratefully acknowledge funding for this research by the U.S. National Science Foundation's Growing Convergence Research program.

REFERENCES

Abrahams, A.C., Dendooven, A., van Der Veer, J.W., Wientjes, R., Toorop, R.J., Bleys, R.L., Hendrickx, A.P., van Leeuwen, M.S., de Lussanet, Q.G., Verhaar, M.C., et al. (2019). Direct comparison of the thickness of the parietal peritoneum using peritoneal biopsy and ultrasonography of the abdominal wall in patients treated

with peritoneal dialysis. Peritoneal Dialysis International, 39(5), 455–464.

Albanese, A.M., Albanese, E.F., Miño, J.H., Gómez, E., Gómez, M., Zandomeni, M., and Merlo, A.B. (2009). Peritoneal surface area: measurements of 40 structures covered by peritoneum: correlation between total peritoneal surface area and the surface calculated by formulas. Surgical and radiologic anatomy, 31, 369–377.

Barr, J., Livne, A., Lushkov, G., Vinograd, I., Efrati, Y., Ballin, A., Lahat, E., and Eshel, G. (1994). Peritoneal ventilation: an animal model of extrapulmonary ventilation in experimental adult respiratory distress syndrome. *Pediatric research*, 35(6), 682–684.

Barr, J., Lushkov, G., Strauss, S., Gurevitch, S., Lahat, E., Bistritzer, T., Klin, B., and Eshel, G. (1996). Peritoneal ventilation in rabbits: augmentation of gas exchange with cisapride. *Thorax*, 51(1), 82–86.

Bertini, P., Guarracino, F., Falcone, M., Nardelli, P., Landoni, G., Nocci, M., and Paternoster, G. (2022). Ecmo in covid-19 patients: a systematic review and meta-analysis. *Journal of Cardiothoracic and Vascular Anesthesia*, 36(8), 2700–2706.

Cameron, M.H., Monroe, L.G., and Peterson, B.K. (2007). Chapter 22- Vital Signs, 598–624. Elsevier Saunders.

Carr, S.R., Cantor, J.P., Rao, A.S., Lakshman, T.V., Collins, J.E., and Friedberg, J.S. (2006). Peritoneal perfusion with oxygenated perfluorocarbon augments systemic oxygenation. *Chest*, 130(2), 402–411.

Collins, J.A., Rudenski, A., Gibson, J., Howard, L., and O'Driscoll, R. (2015). Relating oxygen partial pressure, saturation and content: the haemoglobin-oxygen dissociation curve. *Breathe*, 11(3), 194–201.

Dasta, J.F., McLaughlin, T.P., Mody, S.H., and Piech, C.T. (2005). Daily cost of an intensive care unit day: the contribution of mechanical ventilation. *Critical care medicine*, 33(6), 1266–1271.

Feshitan, J.A., Legband, N.D., Borden, M.A., and Terry, B.S. (2014). Systemic oxygen delivery by peritoneal perfusion of oxygen microbubbles. *Biomaterials*, 35(9), 2600–2606.

Fischbach, M., Dheu, C., Helms, P., Terzic, J., Michallat, A.C., Laugel, V., Wolff-Danner, S., and Haraldsson, B. (2005). The influence of peritoneal surface area on dialysis adequacy. *Peritoneal dialysis international*, 25(3_suppl), 137–140.

Gallet, R., Violle, C., Fromin, N., Jabbour-Zahab, R., Enquist, B.J., and Lenormand, T. (2017). The evolution of bacterial cell size: the internal diffusion-constraint hypothesis. *The ISME journal*, 11(7), 1559–1568.

Grasselli, G., Cattaneo, E., Florio, G., Ippolito, M., Zanella, A., Cortegiani, A., Huang, J., Pesenti, A., and Einav, S. (2021). Mechanical ventilation parameters in critically ill covid-19 patients: a scoping review. *Critical Care*, 25, 1–11.

Haribhai, S. and Mahboobi, S.K. (2022). Ventilator complications. In *StatPearls [Internet]*. StatPearls Publishing.

Hatoum, L. (2016). Diffusion modeling and device development for peritoneal membrane oxygenation.

Iqbal, Q., Younus, M.M., Ahmed, A., Ahmad, I., Iqbal, J., Charoo, B.A., and Ali, S.W. (2015). Neonatal mechanical ventilation: Indications and outcome. *Indian* journal of critical care medicine: peer-reviewed, official

- publication of Indian Society of Critical Care Medicine, 19(9), 523.
- Jägers, J., Wrobeln, A., and Ferenz, K.B. (2021). Perfluorocarbon-based oxygen carriers: from physics to physiology. Pflügers Archiv-European Journal of Physiology, 473, 139–150.
- Katakam, A. (2022). Hill coefficient: Mcat test prep (simple). URL https://www.inspiraadvantage.com. Accessed on April 4, 2023.
- Klein, J., Faithfull, N.S., Salt, P.J., and Trouwborst, A. (1986). Transperitoneal oxygenation with fluorocarbons. *Anesthesia & Analgesia*, 65(7), 734–738.
- Klingenberg, C., Wheeler, K.I., McCallion, N., Morley, C.J., and Davis, P.G. (2017). Volume-targeted versus pressure-limited ventilation in neonates. *Cochrane Database of Systematic Reviews*, (10).
- Leow, M.K.S. (2007). Configuration of the hemoglobin oxygen dissociation curve demystified: a basic mathematical proof for medical and biological sciences undergraduates. Advances in physiology education, 31(2), 198–201.
- Mahon, R.T., Ciarlone, G.E., Roney, N.G., and Swift, J.M. (2019). Cardiovascular parameters in a swine model of normobaric hypoxia treated with 5-hydroxymethyl-2-furfural (5-hmf). Frontiers in Physiology, 10, 395.
- Matsutani, N., Takase, B., Nogami, Y., Ozeki, Y., Kaneda, S., Maehara, T., Kikuchi, M., and Ishihara, M. (2010). Efficacy of peritoneal oxygenation using a novel artificial oxygen carrier (trm-645) in a rat respiratory insufficiency model. Surgery today, 40, 451–455.
- Mishra, V., Svennevig, J.L., Bugge, J.F., Andresen, S., Mathisen, A., Karlsen, H., Khushi, I., and Hagen, T.P. (2010). Cost of extracorporeal membrane oxygenation: evidence from the rikshospitalet university hospital, oslo, norway. European journal of cardio-thoracic surgery, 37(2), 339–342.
- Mohammed, R.U.R., Zollinger, N.T., McCain, A.R., Romaguera-Matas, R., Harris, S.P., Buesing, K.L., Borden, M.A., and Terry, B.S. (2022). Testing oxygenated microbubbles via intraperitoneal and intrathoracic routes on a large pig model of lps-induced acute respiratory distress syndrome. *Physiological Reports*, 10(17), e15451.
- Ohshimo, S. (2021). Oxygen administration for patients with ards. *Journal of Intensive Care*, 9(1), 1–14.
- Reiterer, F., Resch, E., Haim, M., Maurer-Fellbaum, U., Riccabona, M., Zobel, G., Urlesberger, B., and Resch, B. (2018). Neonatal extracorporeal membrane oxygenation due to respiratory failure: a single center experience over 28 years. Frontiers in Pediatrics, 6, 263.
- Rhodes, C.E. and Varacallo, M. (2019). Physiology, oxygen transport.
- Rubenfeld, G.D., Caldwell, E., Peabody, E., Weaver, J., Martin, D.P., Neff, M., Stern, E.J., and Hudson, L.D. (2005). Incidence and outcomes of acute lung injury. New England Journal of Medicine, 353(16), 1685–1693.
- Rycus, P. and Stead, C. (2022). Extracorporeal life support organization registry report 2022. Journal of Cardiac Critical Care TSS, 6(02), 100–102.
- Solass, W., Horvath, P., Struller, F., Königsrainer, I., Beckert, S., Königsrainer, A., Weinreich, F.J., and Schenk, M. (2019). Functional vascular anatomy of the peritoneum in health and disease. *Pleura and peri-*

- toneum, 1(3), 145-158.
- Stentz, M.J., Kelley, M.E., Jabaley, C.S., O'Reilly-Shah, V., Groff, R.F., Moll, V., and Blum, J.M. (2019). Trends in extracorporeal membrane oxygenation growth in the united states, 2011–2014. ASAIO Journal, 65(7), 712– 717.
- Stewart, J.M. and Montgomery, L.D. (2005). Reciprocal splanchnic-thoracic blood volume changes during the valsalva maneuver. *American Journal of Physiology-Heart and Circulatory Physiology*, 288(2), H752–H758.
- Teijeiro-Paradis, R., Gannon, W.D., and Fan, E. (2022). Complications associated with venovenous extracorporeal membrane oxygenation—what can go wrong? Critical Care Medicine, 50(12), 1809–1818.
- van Gelder, M.K., de Vries, J.C., Simonis, F., Monninkhof, A.S., Hazenbrink, D.H., Ligabue, G., Giovanella, S., Joles, J.A., Verhaar, M.C., Bajo Rubio, M.A., et al. (2020). Evaluation of a system for sorbent-assisted peritoneal dialysis in a uremic pig model. *Physiological Reports*, 8(23), e14593.
- Van Milgen, J., Noblet, J., Dubois, S., and Bernier, J.F. (1997). Dynamic aspects of oxygen consumption and carbon dioxide production in swine. *British Journal of Nutrition*, 78(3), 397–410.
- Van Ommen, C.H., Neunert, C.E., and Chitlur, M.B. (2018). Neonatal ecmo. Frontiers in medicine, 5, 289.
- Walters, E.M. and Prather, R.S. (2013). Advancing swine models for human health and diseases. *Missouri Medicine*, 110(3), 212.
- Wunsch, H., Linde-Zwirble, W.T., Angus, D.C., Hartman, M.E., Milbrandt, E.B., and Kahn, J.M. (2010). The epidemiology of mechanical ventilation use in the united states. *Critical care medicine*, 38(10), 1947–1953.
- Zhang, J., Wang, X., Wang, L., Xu, B., and Zheng, M. (2010). Effect of oxygenation of transperitoneal ventilation on the death time after asphyxiation in rabbits. *Minerva anestesiologica*, 76(11), 913–917.
- Zosky, G.R. (2015). Aging of the normal lung. Comparative Biology of the Normal Lung, 185–204.